

WEB-BASED IMPLEMENTATION OF FAST DAM BREAK FLOOD MODELING CAPABILITIES

Mustafa S. Altinakar, PhD ¹
Enrique E. Matheu, PhD ²
Vijay P. Ramalingam ³
Marcus Z. McGrath ⁴
Jun Z. Zou, PE ⁵

ABSTRACT

The Dams Sector Analysis Tool (DSAT) is a web-based tool that provides secure access to different modules and applications covering a wide range of analytical capabilities. In particular, DSAT provides access to the advanced flood modeling capabilities developed by the National Center for Computational Hydroscience and Engineering of the University of Mississippi (UM-NCCHE). Implementation of this capability is the result of a joint effort between UM-NCCHE and the U.S. Department of Homeland Security (DHS), Office of Infrastructure Protection. The flood modeling computational tools were developed at UM-NCCHE through the support provided by the DHS-sponsored Southeast Region Research Initiative Program at the Oak Ridge National Laboratory.

A graphical user interface implemented on DSAT allows the user to provide only the minimum amount of basic information required to set up a simulation scenario. The input data file is sent securely to a computer server at the UM-NCCHE, which hosts two different solvers. The first solver, CCHE2D-FLOOD, uses a robust and accurate first-order, shock-capturing finite volume scheme to solve full dynamic shallow water equations governing the flow of flood waters over complex topography. The second solver, WGFEM, uses GPGPU (General Purpose Graphics Processing Unit) technology to achieve unprecedented computational speeds, which can be as much as 30 to 100 times the computational speed that can be achieved on classical CPU-based numerical models of the same type. Both solvers can handle mixed flow regimes (subcritical, transcritical, supercritical) and wetting and drying. Once the simulation is completed, the shape files representing the flood depth and flood arrival-time grids can be uploaded on the DSAT viewer. The paper describes the implementation efforts and discusses future development plans.

¹ Director and Research Professor, National Center for Computational Hydroscience and Engineering, The University of Mississippi, Oxford, MS 38677.

² Chief, Dams Sector Branch, Sector-Specific Agency Executive Management Office, Office of Infrastructure Protection, U.S. Department of Homeland Security, Washington, DC 20598.

³ Graduate Student, National Center for Computational Hydroscience and Engineering, The University of Mississippi, Oxford, MS 38677.

⁴ Graduate Student, National Center for Computational Hydroscience and Engineering, The University of Mississippi, Oxford, MS 38677.

⁵ Civil Engineer, Dams Sector Branch, Sector-Specific Agency Executive Management Office, Office of Infrastructure Protection, U.S. Department of Homeland Security, Washington, DC 20598.

1. Introduction

In the current state of practice, dam break studies are mostly carried out using one-dimensional models. This generally requires the services of an experienced engineering company as well as the surveying of the cross section data downstream of the dam, which may be quite costly. One dimensional flood simulation results need to be converted to a two-dimensional depth grid for consequence analysis. This process is quite time consuming and involves interpolation based on a digital elevation model (DEM).

Until very recently, two dimensional models were costly and time consuming to use both from the point of data preparation and simulation time. Recent developments in computer hardware and upwind numerical methods with shock capturing capability has completely changed this outlook and made it possible to simulate mixed regime dam-break floods over complex natural topography with wetting and drying in faster-than-real-time speeds. The recent developments in GIS and remote sensing technologies and data layers can now be used to prepare input data for two-dimensional models in a relatively effortless manner.

The present paper presents a first effort to enable dam owners, dam safety and dam security professionals, flood plain managers, and emergency responders who are not necessarily numerical modeling specialists to carry out dam break simulations by providing minimum amount of basic information required to set up a simulation scenario. Funded by the DHS-sponsored Southeast Region Research Initiative (SERRI) Program at the Oak Ridge National Laboratory, UM-NCCHE has developed the capability of preparing and running first-tier dam-break simulations automatically. This capability is made available to Dams Sector stakeholders through the Dams Sector Analysis Tool (DSAT), which is a web-based tool that provides secure access to different analysis modules and applications. The user prepares the basic input data using the DSAT Viewer, which is a graphical user interface. The data defining the scenario to be simulated is automatically transmitted by email to a server running at NCCHE. Special procedures developed by NCCHE allow the preparation of the computational domain and the input data fully automatically without any human intervention. The simulations are carried out on the NCCHE server using a multi-core, multi-threaded implementation of the software. The simulation results (including flood depth maps and arrival time maps) are sent to the DSAT as shape files for viewing and analyzing on the DSAT Viewer.

Section 2 presents various forms of the two-dimensional shallow water equations, which govern flood propagation over complex real terrain. The DSS-WISE software, which forms the basis for the DSAT-DSS-WISE link for automatic dam break flood simulation is briefly described in Section 3. The challenges involved in the numerical solution of shallow water equations are discussed and the numerical schemes used in the CCHE2D-FLOOD model are explained and the data requirements are presented. Finally, Section 4 summarizes the automatic data preparation strategies and methods.

2. Governing Equations for Two-Dimensional Flood Propagation

Two-dimensional shallow water equations (SWE), which describe the unsteady non-uniform overland flow on complex topography, can be written as

$$\frac{\partial h}{\partial t} + \frac{\partial uh}{\partial x} + \frac{\partial vh}{\partial y} = q_v \quad (1a)$$

$$\frac{\partial hu}{\partial t} + \frac{\partial}{\partial x} \left(u^2 h + \frac{1}{2} gh^2 \right) + \frac{\partial uvh}{\partial y} = -ghS_{fx} - gh \frac{\partial z_b}{\partial x} \quad (1b)$$

$$\frac{\partial hv}{\partial t} + \frac{\partial uvh}{\partial x} + \frac{\partial}{\partial y} \left(v^2 h + \frac{1}{2} gh^2 \right) = -ghS_{fy} - gh \frac{\partial z_b}{\partial y} \quad (1c)$$

where u and v are the local velocity components in x and y directions, h is the flow depth, z_b the bed elevation, g the gravitational acceleration, and q_v represents the net source/sink discharge (or mass) added without any momentum input. Source terms due to friction in x and y directions are written as:

$$S_{fx} = \frac{un^2 \sqrt{u^2 + v^2}}{h^{4/3}} \quad \text{and} \quad S_{fy} = \frac{vn^2 \sqrt{u^2 + v^2}}{h^{4/3}} \quad (2)$$

Where n is Manning's roughness coefficient.

Equation 1a represents the conservation of mass and Equations 1b and c are the momentum conservation equations in x and y directions. It should be noted that, SWE are obtained by integrating the Reynolds-averaged Navier-Stokes equations over the depth with the help of certain simplifying assumptions, such as the hydrostatic pressure gradient. The depth and velocity varies spatially but at a given location, only an average velocity (or discharge) is defined for the entire depth.

Unit discharges in x and y directions are defined as:

$$Q_x = uh \quad \text{and} \quad Q_y = vh \quad (3)$$

Using these definitions, the Eqs 1a, b, and c can be rewritten as:

$$\frac{\partial h}{\partial t} + \frac{\partial Q_x}{\partial x} + \frac{\partial Q_y}{\partial y} = q_v \quad (4a)$$

$$\frac{\partial Q_x}{\partial t} + \frac{\partial}{\partial x} \left(\frac{Q_x^2}{h} + \frac{1}{2} gh^2 \right) + \frac{\partial}{\partial y} \left(\frac{Q_x Q_y}{h} \right) = -ghS_{fx} - gh \frac{\partial z_b}{\partial x} \quad (4b)$$

$$\frac{\partial Q_y}{\partial t} + \frac{\partial}{\partial x} \left(\frac{Q_x Q_y}{h} \right) + \frac{\partial}{\partial y} \left(\frac{Q_y^2}{2} + \frac{1}{2} gh^2 \right) = -ghS_{fy} - gh \frac{\partial z_b}{\partial y} \quad (4c)$$

SWE can be cast into a single vector equation of the form:

$$\frac{\partial \mathbf{U}}{\partial t} + \frac{\partial \mathbf{F}(\mathbf{U})}{\partial x} + \frac{\partial \mathbf{G}(\mathbf{U})}{\partial y} = \mathbf{S}(\mathbf{U}) \quad (5)$$

In the above equation, \mathbf{U} represents the vector of conserved variables, $\mathbf{F}(\mathbf{U})$ vector of flux terms in x direction, $\mathbf{G}(\mathbf{U})$ vector of flux terms in y direction, and $\mathbf{S}(\mathbf{U})$ vector of source terms. These vectors are defined as:

$$\mathbf{U} = \begin{bmatrix} h \\ Q_x \\ Q_y \end{bmatrix} \quad \mathbf{F} = \begin{bmatrix} Q_x \\ Q_x^2 / h + gh^2 / 2 \\ Q_x Q_y / h \end{bmatrix} \quad \mathbf{G} = \begin{bmatrix} Q_y \\ Q_y Q_x / h \\ Q_y^2 / h + gh^2 / 2 \end{bmatrix} \quad \mathbf{S} = \begin{bmatrix} q_v \\ -ghS_{fx} - gh \frac{\partial z_b}{\partial x} \\ -ghS_{fy} - gh \frac{\partial z_b}{\partial y} \end{bmatrix} \quad (6)$$

For convenience, SWE are sometimes written in a slightly different form by linearizing the pressure terms and transforming them into source terms that appear on the right hand side of the equation, for example:

$$\frac{\partial h}{\partial t} + \frac{\partial uh}{\partial x} + \frac{\partial vh}{\partial y} = q_v \quad (7a)$$

$$\frac{\partial hu}{\partial t} + \frac{\partial u^2 h}{\partial x} + \frac{\partial uvh}{\partial y} = -gh(\partial Z / \partial x) - g \left(un^2 \sqrt{u^2 + v^2} / h^{2/6} \right) \quad (7b)$$

$$\frac{\partial hv}{\partial t} + \frac{\partial uvh}{\partial x} + \frac{\partial v^2 h}{\partial y} = -gh(\partial Z / \partial y) - g \left(vn^2 \sqrt{u^2 + v^2} / h^{2/6} \right) \quad (7c)$$

where Z the water surface elevation. Using the definition of unit discharges given by Equation 3, we can write:

$$\frac{\partial h}{\partial t} + \frac{\partial Q_x}{\partial x} + \frac{\partial Q_y}{\partial y} = q_v \quad (8a)$$

$$\frac{\partial Q_x}{\partial t} + \frac{\partial Q_x^2 / h}{\partial x} + \frac{\partial Q_y Q_x / h}{\partial y} = -gh(\partial Z / \partial x) - g \left(un^2 \sqrt{u^2 + v^2} / h^{2/6} \right) \quad (8b)$$

$$\frac{\partial Q_y}{\partial t} + \frac{\partial Q_x Q_y / h}{\partial x} + \frac{\partial Q_y^2 / h}{\partial y} = -gh(\partial Z / \partial y) - g \left(vn^2 \sqrt{u^2 + v^2} / h^{2/6} \right) \quad (8c)$$

Equations 8 can also be cast in the same vector form given by Equation 5. In this case, the vectors are defined as:

$$\mathbf{U} = \begin{bmatrix} h \\ Q_x \\ Q_y \end{bmatrix} \quad \mathbf{F} = \begin{bmatrix} Q_x \\ Q_x^2 / h \\ Q_x Q_y / h \end{bmatrix} \quad \mathbf{G} = \begin{bmatrix} Q_y \\ Q_y Q_x / h \\ Q_y^2 / h \end{bmatrix} \quad \mathbf{S} = \begin{bmatrix} q_v \\ -gh(\partial Z / \partial x) - g \left(un^2 \sqrt{u^2 + v^2} / h^{2/6} \right) \\ -gh(\partial Z / \partial y) - g \left(vn^2 \sqrt{u^2 + v^2} / h^{2/6} \right) \end{bmatrix} \quad (9)$$

No closed form analytical solutions are available for SWE, especially when complex topography and boundary conditions are involved. To simulate flood propagation over a natural terrain, the SWE must be solved numerically.

3. DSS-WISE and Numerical Solution of Shallow Water Equations

3.1 General Description of DSS-WISE

DSS-WISE is an integrated software package, designed for water infrastructural safety studies. It can be used to simulate dam/levee breach floods, fluvial floods, storm/tidal surges, landslide waves, and their consequences. It was developed by a team of NCCHE researchers under the DHS-sponsored SERRI Program, which was monitored by the Oak Ridge National Laboratory.

The DSS-WISE was designed to eliminate scientific and technological gaps of the current flood simulation and flood damage evaluation practice entirely based on one dimensional flood simulation, and to improve current engineering and decision-making practice by providing simulation and analyses capabilities with unprecedented realism and robustness. Referring to Figure 1, the DSS-WISE software consists of four major components, which are briefly explained below.

GIS-based Graphical User Interface: A GIS-based graphical user interface handles file and data management, provides access to the remaining three components of DSS-WISE. It has been designed as an add-on extension to ArcGIS, a widely used GIS software package developed and commercialized by ESRI. It provides full GIS connectivity and all functionalities are accessible via dedicated toolbars of the modules. The graphical user interface manages the data files. It checks all the input files generated by the preprocessor for consistency and compatibility and provides user with a dialog window to set the simulation control file.

GIS-based Pre-Processor: The pre-processor allows the user to prepare the input data based on DEM (Digital Elevation Model) files, satellite imagery, classified remote sensing data of land use land cover, and other data defining the physical world and the scenario to be simulated. All operations are carried out directly in ArcGIS platform. The pre-processor functionalities are accessible via a floating toolbar with drop-down menus. In addition to pre-processor functionalities, the user has full access all standard

ArcGIS functionalities. Using the pre-processor, the user can prepare the computational mesh, which can be a DEM, project cut-lines onto the computational domain to represent linear terrain features or a river for coupled 1D-2D modeling, include sources and sinks as well as source-sink pairs to represent controlled release operations and/or flow through structures, and define observation points, lines and profiles for extracting solution results at chosen locations and along a polyline defined by the user.

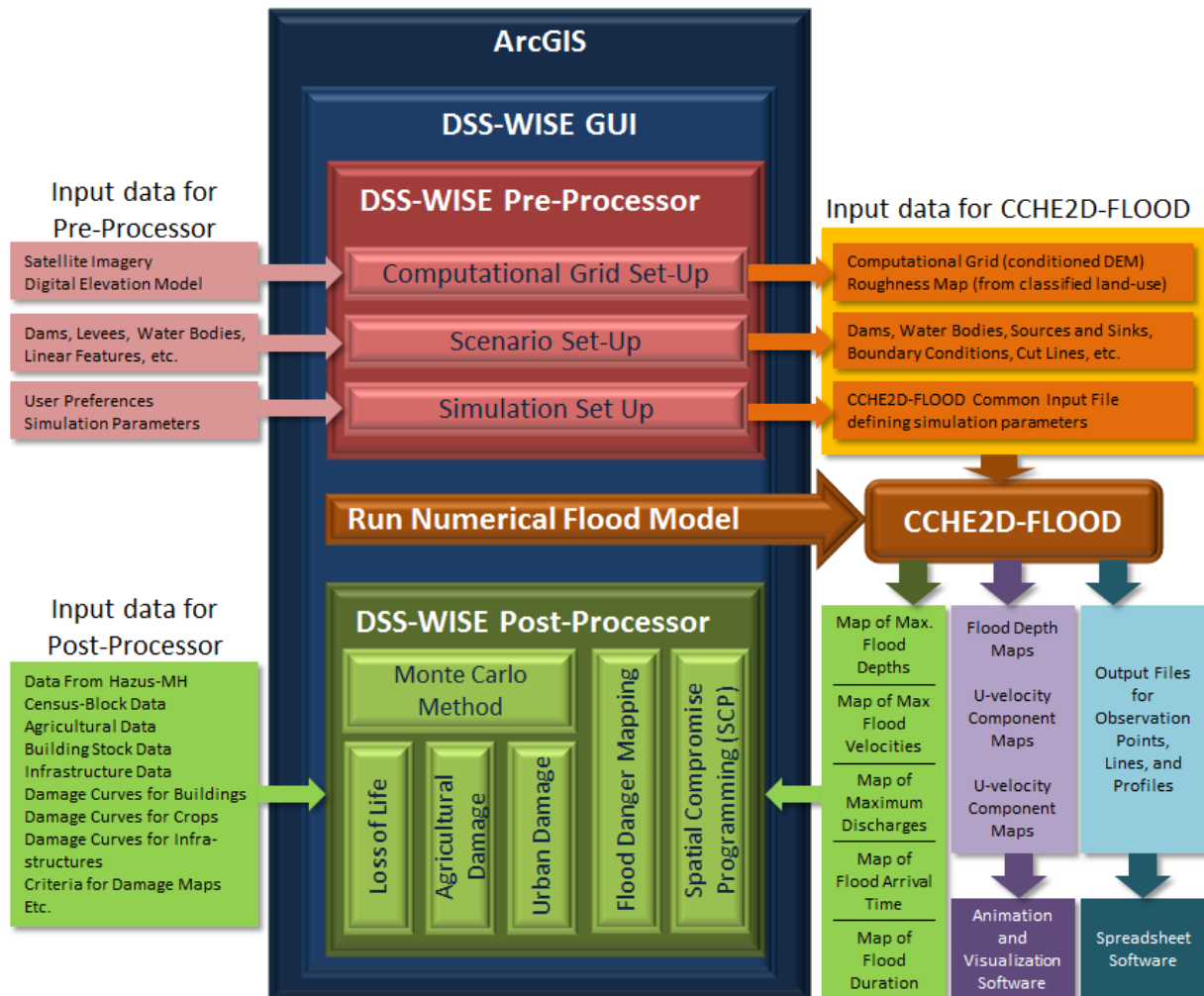


Figure 1. Components of the DSS-WISE integrated software and flow of information.

Two-Dimensional Numerical Flood Simulation Model: A two-dimensional (2D) numerical model, called CCHE2D-FLOOD, which solves SWE over complex natural topography using two different first-order, finite-volume, shock-capturing schemes. CCHE2D-FLOOD can handle mixed flow regimes and wetting/drying. In addition, CCHE2D-FLOOD can use a Digital Elevation Model (DEM) directly as a computational mesh and, thus, avoids the time consuming process of mesh generation and provides direct connectivity with GIS applications. It has several unique features that make it particularly suited for engineering studies:

- A two-sided cut-cell technique that uses ghost fluid has been implemented to represent linear terrain features (such as road and railroad embankments) that

may not be resolved by the DEM but are likely to affect the propagation of the flood wave. The linear features can be projected onto the computational grid from a GIS xyz polyline shape layer.

- Coupled 1D-2D simulation capability is implemented using a variant of the two-sided cut-cell technique. Using this feature one can run levee breach scenarios.
- The user can define sources and sinks as well as sink/source pairs that can be used to define control releases, reservoir operations, and operation of various hydraulic structures or components, such as bridges, culverts, pump stations, etc.
- Different types of boundary conditions can be defined along the edges of the computational domain to represent realistic flow conditions. These include open boundary, wall boundary, prescribed surface elevation or depth boundary, and prescribed inlet discharge boundary.

GIS-based Post-Processor: The numerical model provides a series of output files:

- maps of flow depths over the entire computational mesh at prescribed times;
- maps of velocity components in x and y directions over the entire computational mesh at prescribed times;
- map of maximum depth values over the entire computational mesh;
- maximum velocity vectors for the entire computational mesh;
- map of flood arrival time over the entire computational mesh; and
- map of flood duration times over the entire computational mesh.

These raster files can be directly imported into ArcGIS for post-treatment. The output files can be directly used by HAZUS-MH for consequence analysis. The post processor capabilities implemented in DSS-WISE allow the user to prepare flood depth, flood arrival time and flood duration maps over any type of background, including satellite images. A special module provides the possibility of preparing flood danger maps to humans, vehicles and structures using the criteria established by US Army Corps of Engineers (USACE 1985) or RESCDAM (2000). The postprocessor provides the user with the capability of interfacing the numerical simulation results from CCHE2D-FLOOD with various types of geo-spatial data to evaluate potential loss-of-life using the USBR procedure developed by Graham (1999), potential agricultural damage using the procedures developed by USDA-NRCS, etc.

The link with the DSAT uses mainly the 2D numerical model CCHE2D-FLOOD and some of the modules of the pre-processor, which are reprogrammed to work in an automatic mode rather than the manual mode preferred in the GIS-based pre-processor. From here on, the discussion of DSS-WISE will be restricted to those components that are relevant to the implementation of the link with DSAT.

3.2 CCHE2D-FLOOD and Numerical Solution of SWE

The CCHE2D-FLOOD solves the SWE over a complex natural topography using a finite volume discretization. The computational domain is a regular Cartesian grid in $x-y$ plane, such as the one represented on the left side of Figure 2. A DEM (Digital

Elevation Model) can be directly used as a computational grid. The cell centers are located at (i, j) intersections. The intercell boundaries with the east and west neighbor cells are located at the mid-distance between cell centers and denoted by, $(i+1/2, j)$ and $(i-1/2, j)$, respectively. Similarly, the intercell boundaries with the north and south neighbor cells are located at the mid distance between the cell-centers and denoted by, $(i, j+1/2)$ and $(i, j-1/2)$, respectively.

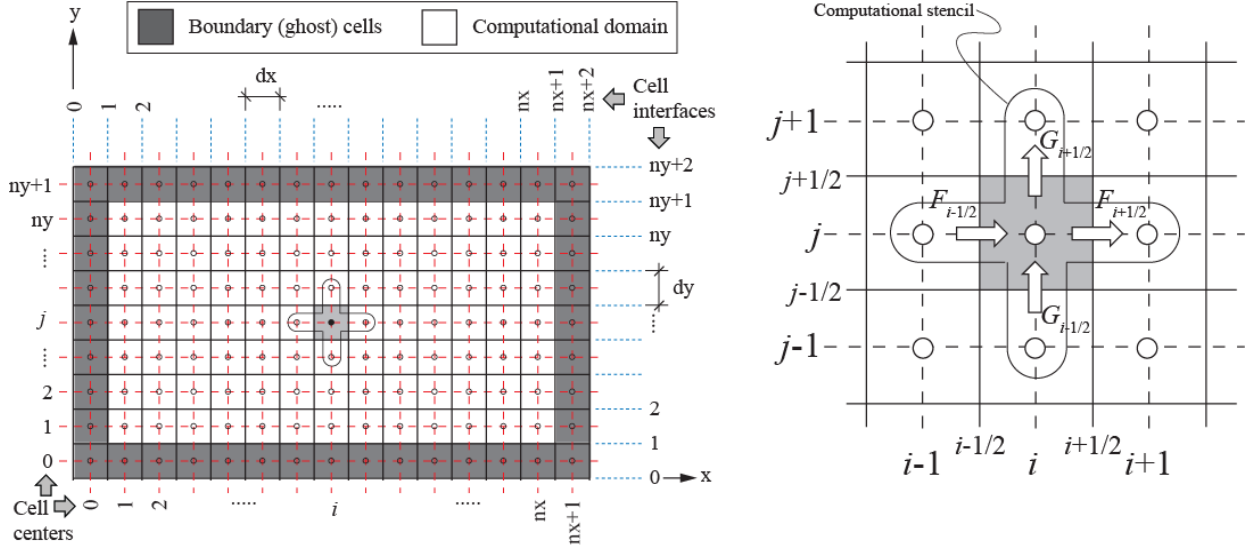


Figure 2. Cartesian computational mesh and the computational stencil used in CCHE2D-FLOOD (taken from Altinakar et al. 2009).

The enlarged view of a typical computational cell (i, j) is represented on the right side of Figure 2. CCHE2D-FLOOD assumes a cell-centered representation. The bed elevation, flow depth (or water surface elevation), and velocity components in x and y directions (or discharge components in x and y directions) are all represented at the center of the cell with sides Δx (or dx) and Δy (or dy). The finite volume discretization of the vector form of SWE is obtained by integrating Equation 5 over a computational cell (i, j) of $\Delta x \times \Delta y$, and taking the time step to be Δt :

$$U_{ij}^{n+1} = U_{ij}^n - \left(\frac{\Delta t}{\Delta x} \right) (F_{i+1/2, j} - F_{i-1/2, j}) - \left(\frac{\Delta t}{\Delta y} \right) (G_{i, j+1/2} - G_{i, j-1/2}) + \Delta t S_{ij} \quad (10)$$

Equation 10 provides a relationship to compute the vector of independent variables in the cell (i, j) at the time step $n+1$, U_{ij}^{n+1} , based on the vector of independent variables in the cell (i, j) at the time step n , U_{ij}^n , as well as the fluxes through east and west intercell boundaries, $F_{i+1/2, j}$ and $F_{i-1/2, j}$, and the north and south intercell boundaries, $G_{i, j+1/2}$ and $G_{i, j-1/2}$. Referring to the enlarged view of the cell on the right hand side of Figure 2, the vectors of independent variables (U_{ij}^{n+1} and U_{ij}^n) are defined at the cell

centers whereas the intercell flux terms ($F_{i+1/2,j}, F_{i-1/2,j}, G_{i,j+1/2}, G_{i,j-1/2}$) are defined at the respective intercell boundaries.

To develop an explicit numerical scheme it is necessary to formulate the intercell flux terms in terms of the values of the independent variables at cell centers, which are known at the time step n . This is a challenging task given that the SWE belong to the family of nonlinear hyperbolic partial differential equations. Numerical solution of these types of equations requires consideration of various issues. A large body of work in theoretical and applied mathematics has been devoted to this subject, which is beyond the scope of this paper. Without going into details, the important properties the numerical scheme should have are briefly discussed below in order to clarify the choices made in the development of the CCHE2D-FLOOD. A more detailed summary can be found in Altinakar et al. (2009).

The solutions of hyperbolic equations, thus the solutions of SWE, are wave-like. A perturbation at a given point propagates in the solution space as a function of time and carries the information. The flow regime (subcritical, supercritical or transcritical) affects the direction of propagation of the information by these waves. The dam/levee breach type flows are generally highly unsteady flows, in which all types of flow regimes occur simultaneously. It is recommended that the solution algorithm should have the **upwind property**, to deal with mixed flow regimes in a simulation. This means that the intercell flux terms in Equation 10 should be computed taking into account the direction and speed of the perturbation waves carrying information over the solution space.

Another important characteristic of SWE equations is that, even smooth initial perturbations (conditions) may transform into discontinuities. For SWE, the discontinuities are positive waves, such as surge waves, hydraulic jumps, etc. It is important that the solution algorithm can capture these discontinuities and propagate them accurately without numerical dissipation. Thus, one must use a **shock-capturing** scheme, which is free of oscillations near the sharp discontinuities and has minimal numerical dissipation. In order to do so, the equations must be written in conservation form, rather than divergence form. Vector form of SWE given by Equation 5 using either the vectors defined by Equation 6 or Equation 9 are in conservation form.

The solutions of SWE can sometimes produce non-physical solutions that do not satisfy the entropy condition. Numerical scheme used for SWE should either be **entropy satisfying** or additional **entropy-fix** algorithms must be included to avoid non-physical solutions.

In dam/levee break/breaching type floods initially dry areas may become flooded and flooded areas can become dry. The numerical solution algorithm must, therefore, be able to handle **wetting/drying** fronts.

CCHE2D-FLOOD proposes two different first-order shock-capturing upwind schemes for the formulation of intercell fluxes in Equation 10: (1) first order upwind scheme; and

(2) first-order HLLC scheme. Implementation of these two schemes in CCHE2D-FLOOD is briefly described in the following subsections.

3.2.1 First-order upwind scheme

This implementation adopts the formulation of fluxes and the source terms as given by Equation 9. The first order upwind scheme consists of using the information based on the direction of the flow. The intercell fluxes in Equation 10 are computed using the following expressions:

$$\mathbf{F}_{i+1/2j} = \begin{bmatrix} Q_x \\ Q_x^2/h \\ Q_x Q_y/h \end{bmatrix}_{i+k} \quad k = \begin{cases} 0 & Q_x \geq 0 \\ 1 & Q_x \leq 0 \end{cases} \quad (11a)$$

$$\mathbf{G}_{ij+1/2} = \begin{bmatrix} Q_y \\ Q_y Q_x/h \\ Q_y^2/h \end{bmatrix}_{j+m} \quad m = \begin{cases} 0 & Q_y \geq 0 \\ 1 & Q_y \leq 0 \end{cases} \quad (11b)$$

The source term on the right hand side of Equation 10 is given by:

$$\mathbf{S} = \begin{bmatrix} q_v \\ -gh_{ij}^{n+1} \left[\left(\frac{\partial Z}{\partial x} \right) - g \frac{u_{ij} \sqrt{u_{ij}^2 + v_{ij}^2}}{(h_{ij}^{1/6}/n)^2} \right] \\ -gh_{ij}^{n+1} \left[\left(\frac{\partial Z}{\partial y} \right) - g \frac{v_{ij} \sqrt{u_{ij}^2 + v_{ij}^2}}{(h_{ij}^{1/6}/n)^2} \right] \end{bmatrix} \quad (12)$$

In which the gradient of the water surface elevation is computed using the following expression:

$$\frac{\partial Z}{\partial x} = \begin{cases} Z_{i+1,j} - Z_{i,j} & \text{if } (Q_x)_{i,j} > 0 \text{ and } (Q_x)_{i+1,j} > 0 \\ Z_{i,j} - Z_{i-1,j} & \text{if } (Q_x)_{i,j} < 0 \text{ and } (Q_x)_{i-1,j} < 0 \\ (Z_{i+1,j} - Z_{i-1,j})/2 & \text{all other cases} \end{cases} \quad (13)$$

In order to avoid tracking the wet/dry interface and using special algorithms, the implementation in CCHE2D-FLOOD assumes that the terrain is covered by a very thin layer of water. When the water is equal to or smaller than this depth the terrain is assumed to be dry and the velocity components at the cell center are set to zero. This

trick eliminates the need for a special treatment for wetting and drying. It is important to keep the thickness of this initial layer as small as possible in order not to influence the wave speeds. In CCHE2D-FLOOD the default value of the thickness of the layer covering the entire domain is taken as 10^{-8} m, which is very small and does not affect the wave speeds.

The explicit computation of the next time step value for a given cell using Equation 10 with first-order upwind flux involves only the known values of the independent variables in the cell itself and in its immediate neighbors to the east, west, north, and south. The computational stencil, which looks like a '+' sign, is depicted on the right hand side of Figure 2.

3.2.2 First-order HLLC scheme

In finite volume modeling, the independent variables (h, Q_x, Q_y) are defined as an integral average value over each cell. This leads to discontinuities in the values of the primitive variables across neighboring cells. Godunov (1976) introduced the idea of computing the intercell fluxes by solving a generalized Riemann problem (GRP) at each cell interface (see Altinakar et al. 1999), where the discontinuous values of the primitive variables on the left and right sides of the interface are used as the initial discontinuous data. Exact solution of GRP is time consuming and rarely used in numerical models. Various approximate methods have been proposed to solve the GRP at cell interfaces.

Harten, Lax and van Leer (1983) developed direct approximations to Riemann solver for computing Godunov fluxes at the computational cell interfaces. This became known as HLL Riemann solver. The HLL Riemann solver is quite simple and satisfies the entropy; thus, no entropy fix is needed. On the other hand the HLL is only valid for one dimensional flows defined by two equations. Two dimensional solution of SWE involves three equations. Toro et al. (1992 and 1994) modified HLL solver to include an intermediate wave, called contact wave. The modified method is called HLLC Riemann solver, where C stands for the contact wave. Detailed description of the HLL and HLLC methods and the associated derivations can be found in various textbooks (Toro, 2010).

Implementation of the HLLC numerical scheme in CCHE2D-FLOOD follows the methodology presented in Kim et al. (2007). We adopt the vector form of SWE as described by Equation 5 where the flux terms are given by Equation 6.

To compute the numerical HLLC fluxes, the depth and velocities left and right of the cell interface are used to determine the wave speeds. These wave speeds are used to determine which of the four states to use to compute the fluxes. The wave speeds are given by:

$$\text{If the left state is dry: } \begin{cases} S_L = u_R - 2\sqrt{gh_R} \\ S^* = S_L \\ S_R = u_R + \sqrt{gh_R} \end{cases} \quad (14a)$$

$$\text{If the right state is dry:} \quad \begin{cases} S_L = u_L - 2\sqrt{gh_L} \\ S^* = S_R \\ S_R = u_L + \sqrt{gh_L} \end{cases} \quad (14a)$$

$$\text{Otherwise:} \quad \begin{cases} S_L = \min(u_L - \sqrt{gh_L}, u_* - \sqrt{gh^*}) \\ S^* = u_* = \frac{u_L + u_R}{2} + \sqrt{gh_L} - \sqrt{gh_R} \\ S_R = \max(u_R + \sqrt{gh_R}, u_* + \sqrt{gh^*}) \end{cases} \quad (14a)$$

where

$$h^* = \frac{1}{g} \left[\frac{1}{2} (\sqrt{gh_L} + \sqrt{gh_R}) + \frac{1}{4} (u_L - u_R) \right]^2 \quad (15)$$

Based on the wave speeds given by Equation 14, the intercell flux can be directly computed from one of the four expressions given below:

$$\mathbf{f} = \begin{cases} \mathbf{f}_L & \text{if } 0 \leq S_L \\ \mathbf{f}_L^* = \mathbf{f}_L + S_L (U_L^* - u_L) & \text{if } S_L \leq 0 \leq S^* \\ \mathbf{f}_R^* = \mathbf{f}_R + S_R (U_R^* - u_R) & \text{if } S^* \leq 0 \leq S_R \\ \mathbf{f}_R & \text{if } S_R \leq 0 \end{cases} \quad (16)$$

where

$$U_K^* = h_K \begin{pmatrix} S_K - u_K \\ S_K - S^* \end{pmatrix} \begin{bmatrix} 1 \\ S^* \\ v_K \end{bmatrix} \quad \text{with} \quad K = L, R \quad (17)$$

As it can be seen, in this implementation the wet/dry interface is considered explicitly and the computations are done accordingly. Therefore, there is no need to define a very thin layer of fluid covering the entire computational domain. In order to take into account all special situations, including those with wet and dry cells, a special procedure is used for calculating the intercell fluxes at the interfaces. Consider the situation depicted in Figure 3. The interface I is located between cells left (L) and right (R). First we define a bed elevation at the interface:

$$z_{bI} = \max(z_{bL}, z_{bR}) \quad (18)$$

Then the temporary values of variables to be used for the left cell (L) in computing the fluxes are found as below:

$$\begin{cases} \text{if} & (h_L + z_{bL} - z_{bI}) > 0 & h_L' = h_L + z_{bL} - z_{bI} \\ \text{else} & & h_L' = u_L' = v_L' = 0 \end{cases} \quad (19)$$

Similarly the temporary values of variables to be used for the left cell (R) in computing the fluxes are found as below:

$$\begin{cases} \text{if} & (h_R + z_{bR} - z_{bI}) > 0 & h_R' = h_R + z_{bR} - z_{bI} \\ \text{else} & & h_R' = u_R' = v_R' = 0 \end{cases} \quad (20)$$

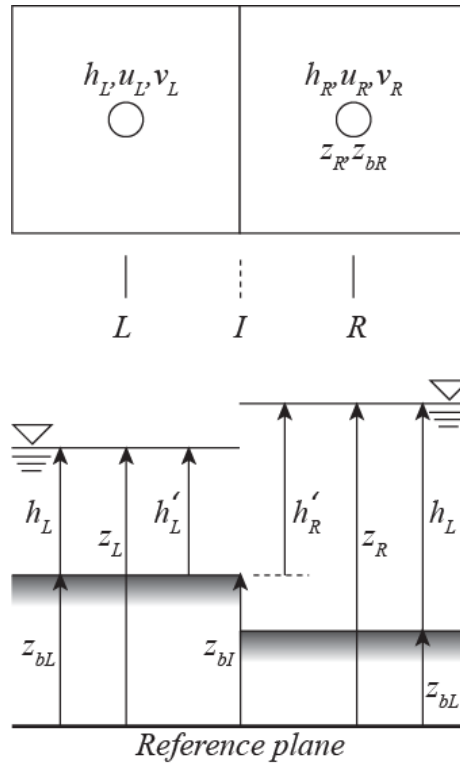


Figure 3. Procedure for the treatment of the wet dry interface.

Computation of the gradients of the bed elevation, which appear in the source terms, also requires a special attention. For the cell (ij), the gradients of bed elevation in x and y directions are carried out using the following expressions:

$$\frac{\partial z_b}{\partial x} = \frac{z_{b_{down}} - z_{b_{up}}}{\Delta x} \quad \text{and} \quad \frac{\partial z_b}{\partial y} = \frac{z_{b_{down}} - z_{b_{up}}}{\Delta y} \quad (21)$$

where the definition of up and down depends on the direction:

$$\text{in } x \text{ direction} \quad \begin{cases} z_{b_{down}} = \min(z_{b_{i+1/2j}}, h_{ij} + z_{b_{ij}}) \\ z_{b_{up}} = \min(z_{b_{i-1/2j}}, h_{ij} + z_{b_{ij}}) \end{cases} \quad (22a)$$

$$\text{in } y \text{ direction} \quad \begin{cases} z_{b_{down}} = \min(z_{b_{ij+1/2}}, h_{ij} + z_{b_{ij}}) \\ z_{b_{up}} = \min(z_{b_{ij-1/2}}, h_{ij} + z_{b_{ij}}) \end{cases} \quad (22b)$$

When in a cell the computed depth is less than or equal to a very small value, say $\varepsilon = 10^{-9}$ m, then it is assumed dry and the velocity components are set to zero.

The explicit computation of the next time step value for a given cell using Equation 10 with the HLLC scheme involves only the known values of the independent variables in the cell itself and in its immediate neighbors to the east, west, north, and south. The computational stencil, which looks like a '+' sign, is depicted on the right hand side of Figure 2.

3.3 Data Requirements

One of the important characteristics of the CCHE2D-FLOOD model is its ability to run with different levels of input data complexity and scenario definition. For the DSAT link, the data requirements are streamlined as much as possible.

The minimum data requirements include:

1. Digital Elevation Model (DEM) of the area of interest where the inundation due to dam break will take place,
2. Locations of bridges that may play an important role in the propagation of the flood,
3. Coordinates of the two points defining the extremities of the dam axis,
4. Coordinates of a point (any point) on the reservoir side of the dam,
5. The elevation of the water surface in the reservoir at the time of the failure of the dam,
6. Manning's roughness coefficient for the inundation area (which can either be a single average value for the entire area of interest or a map showing the variation of the roughness coefficient over the computational domain).

In order to further simplify the task of the user, some additional information on the dam is automatically inserted by the DSAT Viewer on which the input data is prepared by the user. Furthermore, a specialized program residing on a dedicated NCCHE server automatically prepares all the data files needed by the CCHE2D-FLOOD model based on the initial information set provided by the user through the DSAT link. The automatic data generation procedure will be explained in the next section.

4. User Interface and Automatic Preparation of Input Data

4.1 DSAT Viewer for Input Data Preparation

The details regarding the multiple functionalities of the DSAT tool are discussed in a companion paper and will not be repeated here. Only the procedure leading to launching an automatic dam break analysis will be described in this section.

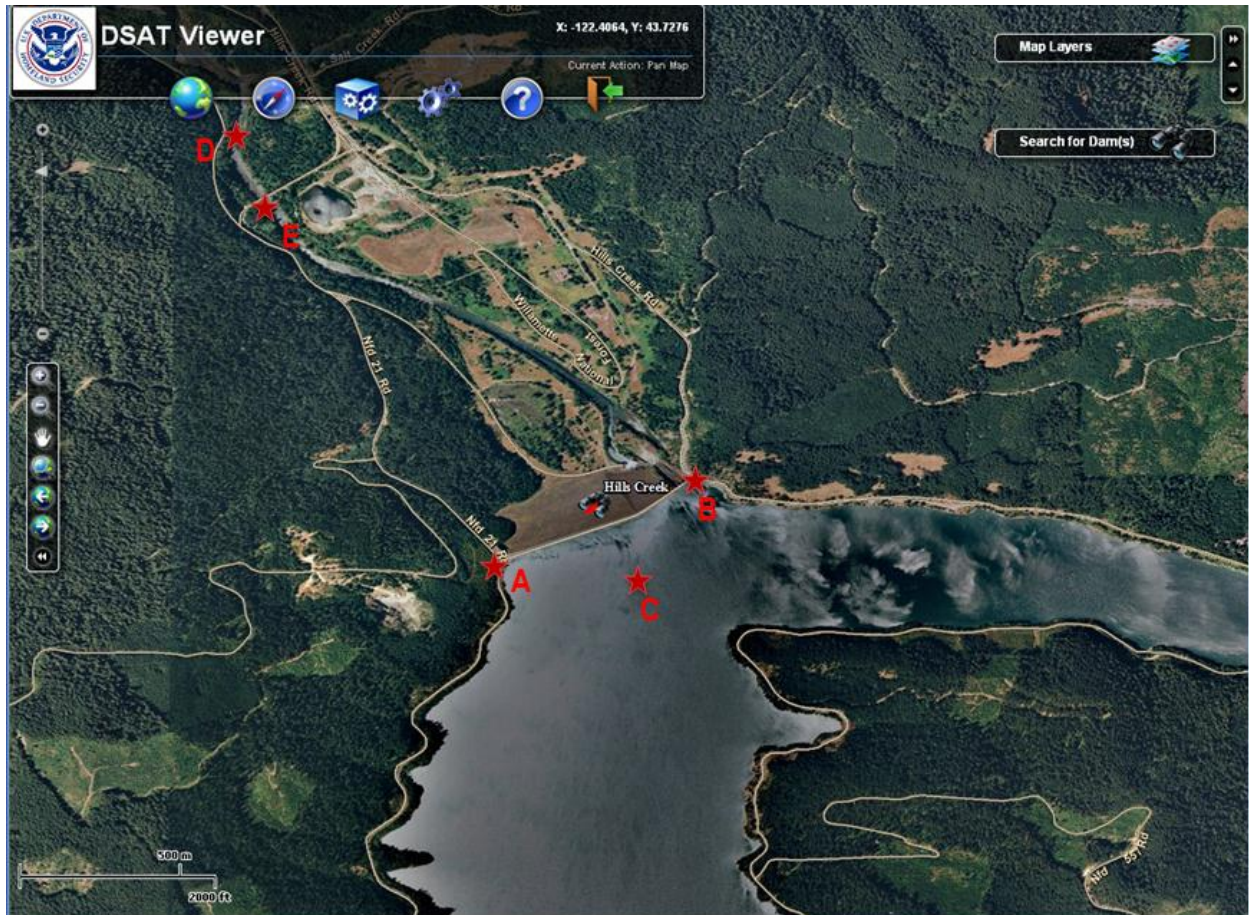


Figure 4. DSAT Viewer and the data items specified by the user.

An accredited user, who wishes to use the DSAT-DSS-WISE capabilities to carry out a dam break analysis, connects to the DSAT portal and signs in using his/her username and password. The DSAT Viewer provides various map layers and a search tool for finding a particular dam. Using the search tool, the user locates the particular dam in which he/she is interested and displays it on the screen as shown in Figure 4.

The DSAT Viewer provides a special tool called “DSS-WISE Prep” which assists the user in providing the data necessary for the dam-break analysis. Before starting a session the user loads the layers showing satellite imagery and the locations of the bridges registered in the National Bridge Inventory (compiled by the Federal Highway Administration, U.S. Department of Transportation). Figure 5 shows a typical session with the DSS-WISE Prep tool in the DSAT Viewer using the example of the preparation of the input data for simulating a dam break scenario for the Dexter Dam in Oregon. At the end of the session, the user can generate an XML file that contains the data required for the simulation. This XML file is sent by email to the UM-NCCE server. The

structure of the XML file is depicted in Figure 6. Most of the data items are self-explanatory. Only some brief comments are provided below to further clarify the data provided

Analysis Name is a distinct name that identifies the particular dam break analysis that will be carried out. Although the user can provide any alphanumeric character string, it is recommended to use a meaningful and clearly identifiable name. In the XML file (Figure 6), this data item is identified by the pair of tags <ModelRunName> and </ModelRunName>.

Project Name is an alphanumeric character string defining the name of the dam for which the analysis is being carried out. In the XML file (Figure 6), this data item is identified by the pair of tags <ProjectName> and </ProjectName>.

Project Description is a short text that describes the simulation to be carried out and its purpose. The length of the text is not limited. In the XML file (Figure 6), this data item is identified by the pair of tags <ProjectDescription> and </ProjectDescription>.

NID ID is the National Inventory of Dams (NID) identification number. In the XML file (Figure 6), this data item is identified by the pair of tags <NIDID> and </NIDID>. As soon as the NID ID is provided by the user, the DSS-WISE Prep tool queries the NID database and extracts the following additional information that is automatically written into the XML file listed in Figure 6.

- Dam Hydraulic Height, which is defined as the vertical difference in feet between the maximum designed water level and the lowest point in the original streambed. In the XML file (Figure 6), this data item is identified by the pair of tags <DamHydHght> and </DamHydHght>.
- Dam NID Height, is a height value in feet calculated based on the Dam Height, Hydraulic Height, and the Structural Height. It provides a single height value to facilitate database queries. In the XML file (Figure 6), this data item is identified by the pair of tags <DamNIDHght> and </DamNIDHght>.
- Dam Height, which is defined as the vertical difference in feet between the lowest point on the crest of the dam and the lowest point in the original streambed. In the XML file (Figure 6), this data item is identified by the pair of tags <DamHght> and </DamHght>.
- NID Storage, is a volume value in acre-feet calculated based on the Normal Storage and the Maximum Storage. It provides a single storage value to facilitate database queries. In the XML file (Figure 6), this data item is identified by the pair of tags <NIDStorage> and </NIDStorage>.
- Normal Storage, which is defined as the total storage space in a reservoir below the normal retention level, including dead and inactive storage and excluding any flood control surcharge storage. In the XML file (Figure 6), this data item is identified by the pair of tags <NormStorage> and </NormStorage>.
- Surface Area, which is defined as the surface area in acres of the impoundment at its normal retention level. In the XML file (Figure 6), this data item is identified by the pair of tags <Surface> and </Surface>.

User's Email Address is an alphanumeric character string defining the email address to which the simulation results are sent accompanied by a short report automatically written and a disclaimer statement. In the XML file (Figure 6), this data item is identified by the pair of tags <UserEmail> and </UserEmail>.

To localize the dam on the DEM that represents the computational domain, the user provides the left and right end coordinates of the dam centerline when looking towards downstream. The coordinates of these two end points, which are defined as points A and B in Figure 4, can be input by clicking their position on the DSAT Viewer. The DSAT Viewer automatically fills in the latitude and longitude of the positions clicked as end points of the dam, and writes them into the XML file. The data items written into the XML file are (see Figure 6):

- **Latitude of the left end** of the dam in decimal degrees, which is identified by the pair of tags <LeftDamLatitude> and </LeftDamLatitude>,
- **Longitude of the left end** of the dam in decimal degrees, which is identified by the pair of tags <LeftDamLongitude> and </LeftDamLongitude>,
- **Latitude of the right end** of the dam in decimal degrees, which is identified by the pair of tags <RightDamLatitude> and </RightDamLatitude>,
- **Longitude of the right end** of the dam in decimal degrees, which is identified by the pair of tags <RightDamLongitude> and </RightDamLongitude>.

In order to define the reservoir, the user is requested to provide the coordinates of a point in the reservoir and the elevation of the water surface in the reservoir at the time of the failure. The user can input the coordinates of the point by clicking any point, which is identified as point C in Figure 4, on the reservoir side of the dam, provided that it is within the area occupied by the water. The coordinates of the positions clicked by the user is automatically recorded and the user is prompted to provide the water surface elevation (in feet with respect to the NAVD 88 mean sea level) in the reservoir at the time of the failure. The data items written into the XML file are (see Figure 6):

- **Latitude of a point (any point) in the lake** in decimal degrees, which is identified by the pair of tags <BehindDamLatitude> and </BehindDamLatitude>,
- **Longitude of a point (any point) in the lake** in decimal degrees, which is identified by the pair of tags <BehindDamLongitude> and </BehindDamLongitude>,
- **Pool elevation in ft** with respect to the NAVD 88 mean sea level, which is identified by the pair of tags <PoolElevation> and </PoolElevation>.

The above items complete the standard information that has to be included in the XML file to be sent to the NCCHE server to initiate the dam break simulation. Depending on the type of the problem, the user may wish to provide additional information regarding the bridges that may act as obstacles to the propagation of the flow and, thus, need to be removed in the DEM based on the width of the bridge opening. The number of bridges that can be specified by the user is not limited. Thus the length of the XML file will depend on the number of bridges entered by the user.


The bridge information is obtained from the National Bridge Inventory layer which must be loaded into the DSAT Viewer. The bridge openings that must be provided in the DEM are identified by clicking on the position of the bridge in the National Bridge Inventory layer. The DSAT Viewer automatically queries the National Bridge Inventory database and writes the following data items into the XML file (see Figure 6):

- **Latitude of the bridge center point** in decimal degrees, which is identified by the pair of tags <Bridge1LocationLatitude> and </Bridge1LocationLatitude>,
- **Longitude of the bridge center point** in decimal degrees, which is identified by the pair of tags <Bridge1LocationLongitude> and </Bridge1LocationLongitude>,
- **Total width of the bridge opening** in decimal feet, which is identified by the pair of tags <Bridge1OpeningLength> and </Bridge1OpeningLength>,

The number of the bridge appearing in the tag is automatically incremented each time a new bridge is defined by the user by clicking its position in the DSAT Viewer.

4.2 Automatic Input Data Preparation on NCCHE Server

The aim of the DSAT-DSS-WISE link is to facilitate access to the advanced flood modeling capabilities developed by UM-NCCHE by providing a first-tier level automatic dam-break flood simulation without any human intervention.

 DSAT Viewer DSS-WISE Prep		
1	Give a name for this particular run	Analysis Name XXX Test Run 01
2	Name of this dam or asset	Project Name Dexter Dam
3	Describe the simulation scenario and purpose briefly	Project Description Dexter Dam Test DSS-WISE Prep
4	ID no of the dam in the National Inventory of Dams (NID)	NID ID OR0006
5	Email address to which the results will be sent	User's Email Address OR00006
6a	Point A: Left end of the dam axis looking towards downstream. Click Point A in the DSAT Viewer or type in latitude and longitude.	Latitude of the left end 43.923181
6b		Longitude of the left end -122.805908
7a	Point B: Right end of the dam axis looking towards downstream. Click Point B in the DSAT Viewer or type in latitude and longitude.	Latitude of the right end 43.924532
7b		Longitude of the right end -122.805339
8a	Point C: Coordinates of a point in the lake impounded by the dam. Click a point in the DSAT Viewer or type in latitude and longitude.	Latitude of a point (any point) in the lake 43.920911
8b		Longitude of a point (any point) in the lake -122.805618
9	Elevation of the water surface in the reservoir during failure	Pool Elevation in ft (NAVD 88, mean sea level) 3210
10a	Bridge 001: Click on the bridge in DSAT Viewer to populate the latitude, longitude and the width of the total bridge opening	Latitude of the bridge center point 44.754101
10b		Longitude of the bridge center point -123.148201
10c		Total width of the bridge opening in ft 200
11a	Bridge 002: Click on the bridge in DSAT Viewer to populate the latitude, longitude and the width of the total bridge opening	Latitude of the bridge center point 43.9253205
11b		Longitude of the bridge center point -122.148201
11c		Total width of the bridge opening in ft 300

Input a Bridge

Write Input File for DSS-WISE

Figure 5. Use of DSS-WISE Prep tool in DSAT Viewer to prepare a dam break simulation.

```

<DSSWISE>
<ModelRunName>XXX test case 0001</ModelRunName>
<ProjectName>Dexter Dam</ProjectName>
<ProjectDescription>Dexter Dam Test DSS-WISE Prep</ProjectDescription>
<NIDID>OR00006</NIDID>
<!-->Dam Hydraulic Height (feet)</!-->
<DamHydHght>60</DamHydHght>
<!-->NID Height (feet)</!-->
<DamNIDHght>66</DamNIDHght>
<!-->Dam Height (feet)</!-->
<DamHght>63</DamHght>
<!-->NID Storage (acre-feet)</!-->
<NIDStorage>29900</NIDStorage>
<!-->Normal Storage (acre-feet)</!-->
<NormStorage>26600</NormStorage>
<UserEmail>Test@dhs.gov</UserEmail>
<LeftDamLatitude>43.923181</LeftDamLatitude>
<LeftDamLongitude>-122.805908</LeftDamLongitude>
<RightDamLatitude>43.924532</RightDamLatitude>
<RightDamLongitude>-122.805339</RightDamLongitude>
<BehindDamLatitude>43.920911</BehindDamLatitude>
<BehindDamLongitude>-122.805618</BehindDamLongitude>
<PoolElevation>3210</PoolElevation>
<Bridge1LocationLatitude>-43.9253205</Bridge1LocationLatitude>
<Bridge1LocationLongitude>-122.148201</Bridge1LocationLongitude>
<Bridge1OpeningLength>200</ Bridge1OpeningLength>
<Bridge2LocationLatitude>-43.9253205</Bridge2LocationLatitude>
<Bridge2LocationLongitude>-122.148201</Bridge2LocationLongitude>
<Bridge2OpeningLength>300</Bridge2OpeningLength>
</DSSWISE>

```

Figure 6. Structure of the XML input data file. Highlighted lines are comment lines.

The tasks that must be carried out by the NCCHE server are (1) detection of a dam-break flood simulation requests arriving at the NCCHE server and queuing of the requests based on the level of priority; (2) preparing all the input files for the CCHE2D-FLOOD model based on the information included in the XML file and the various additional geospatial data layers residing on the server, such as 10m-resolution DEM and 30m-resolution of land-use land-cover map of the entire United States; (3) launching the appropriate version of the CCHE2D-FLOOD model to simulate the propagation of the dam-break flood either until the flood reaches a point 60 miles downstream of the dam or until the propagation of the flood stops or slows down due to emptying of the reservoir, whichever occurs first; (4) preparing a short report, which explains the input data received and the assumptions made during the preparation of the input data files and the issues encountered during the simulation, if any; and (5) emailing the simulation results at selected times of the flood propagation to the email

address provided in the XML file, together with the report and the disclaimer statement. Accomplishing all these tasks automatically is a highly challenging task and required the development of a large number of utility programs written in Python, Visual Basic, and C++ programming languages. These are explained in the following sections.

4.2.1 Job Detection and Scheduling

The XML input file created by the DSAT Viewer is sent to a special email address at NCCHE. A special filter utility checks all the emails arriving at that address keeps only those legitimate email requests sent by the DSAT portal. All other emails arriving at that address are automatically erased.

Valid emails containing job requests are separated and parsed to extract the attachment file, which is uploaded into a dedicated folder. A Python executable code regularly checks the folder for new requests. When a new request is detected, it is first checked for the integrity of its information. If the XML file is found to contain erroneous data, an error message is sent to the DSAT portal and the file is erased from the folder. If no errors are found, the information is copied into the corresponding fields of a dedicated database and the original XML file is erased from the email server.

In addition to the information contained in the XML file, the database stores following additional data fields, which are used for job scheduling and archiving:

- **JOBID:** a unique identification number for the request
- **RDATETIME:** an alphanumeric field containing date and time at which the request was received
- **CDATETIME:** an alphanumeric field containing date and time at which the job was completed
- **SDATETIME:** an alphanumeric field containing date and time at which the job was sent back to DSAT portal
- **JOBSTATUS:** An alphanumeric field that stores the information on the status of the job. At the completion of the job, the completion status is written.
- **JOBWORKSPACE:** the folder where the corresponding input and output files are stored for archiving purposes.
- **JOBPRIORITY:** A numeric value reflecting the priority level given to the job.

The jobs are scheduled according to their priority level and the availability of the computer resources. The computer made available by NCCHE for the DSAT-DSS-WISE link is a 12-core Xeon rack-mount server with 6 terabytes of storage, 24 GB memory and 3 NVIDIA Fermi C2070 6GB CUDA cards. The semi-automatic data preparation requires clipping the computational domain from 10m resolution DEM tiles for the entire USA. This operation involves large files as it will be explained in the next subsection. In order to reduce the processing time, the server is equipped with four 240GB Solid State Drives. The DSS-WISE software is written as a multi-core multithreaded application and can be run on multiple processors to reduce the computational time even when dealing with large domains. As the jobs are queued, the job scheduler makes an evaluation of the computational resources (processor and

memory) available and decides how many processors will be assigned for the job. This takes into account the jobs that are already running and using the computer resources and the jobs that are waiting in the queue. During the completion of the present paper, the DSAT-DSS-WISE link was in testing phase. The actual work load to be expected when it is opened for general use is hard to estimate. Therefore, it is planned to optimize the job scheduler, based on the experience that will be gained once the link is made available to the user community.

4.2.2 Automatic Preparation of the Computational Domain

The 10m-resolution DEM for the entire United States is stored in the NCCHE server. It consists of tiles covering an area of approximately 1/3 arc second in each direction. The tiles contain 10812×10812 cells having a size of 9.2592593e-005 arc second. The file size for a tile is about 450 MB. The entire data set is approximately 450 GB. For computations, the final clipped area is projected using the Universal Transverse Mercator (UTM) coordinate system using the UTM zone based on the location of the center of the dam.

The automatic clipping of the area of interest for a particular dam-break simulation from the 10m-DEM data set and its preparation as computational grid involves multiple challenges. The first challenge concerns the boundaries of the domain to be clipped as the computational domain. A trained person can easily and quickly judge this from the general aspect of the topography and the location of the dam. The task is much more difficult without human intervention. The second challenge is concerned with the fact that that, in general, the DEM does not reflect the true topography that can be used for modeling flood propagation. Although there are also other issues, for the purposes of first-tier modeling adopted in DSAT-DSS-WISE link, three main problem areas must be resolved:

- Often the DEM represents the reservoir water surface rather than its bottom topography. In some cases, it could be possible to obtain the reservoir bottom topography from other sources and incorporate it into the DEM. However, this solution would require human intervention and it could not be adopted in a fully automatic system. The solution adopted in the present case consists of estimation of the bottom topography of the reservoir from the surrounding topography based on the estimated reservoir volume.
- Often, the main body of the dam, at least the crown and the downstream slope, is represented in the DEM. Thus the cells that represent the impounding structure need to be automatically recognized and removed (lowering them to the level of the valley), in order to simulate the breaching or failure of the dam.
- Bridges in a DEM are represented by the elevation of the crown of the deck and, thus, may act as obstacles to the flow. The solution consists of correcting the DEM cells at the location of the bridge to create a passage for the water flow based on the width of the bridge. This operation should be done automatically.

The procedure programmed on the NCCHE Server accomplishes all the tasks automatically and prepares the input files needed to run the CCHE2D-FLOOD model.

The strategy adopted by the program, which consists of assuming first a very large extent and then reducing its size based on a rough preliminary dam-break simulation, can be summarized as follows:

1. The position of the center of the dam axis is computed from the coordinates of the left and right ends of the dam axis given in XML.
2. The initial analysis is concerned with flooding up to a distance of 60 miles from the dam. Therefore, the program calculates the coordinates of the corners of a preliminary computational domain that extends 65 miles in four main directions. All the DEM tiles concerned by this preliminary computational domain are selected. In the worst case scenario, depending on the position of the dam center with respect to the limits of the DEM tiles, 12 tiles of 450MB would be selected.
3. The selected DEM tiles (up to a total of 12 tiles) are mosaicked together at 100 m resolution and projected using the appropriate UTM projection. A preliminary computational domain is then clipped from the projected mosaic at 10m-resolution.
4. A special utility program for bridge removal is run to remove all the bridges given in the XML file.
5. A mock flood simulation is carried with this initial 10m-resolution computational domain to calculate the rough extent of the flow. It is important to mention that this preliminary simulation is not a dam break simulation and does not represent the reservoir. It is more of a filling algorithm based on a water depth specified downstream of the dam. The coordinates of a rectangular area that contains the reservoir and the entire, roughly calculated, inundation area extracted to serve as a better estimation of the extent of the computational domain.
6. Using the corners of the new computational domain obtained from step 5, a new computational grid is clipped from the DEM tiles selected in step 2, by mosaicking them together at either at 10 or 30 meters resolution.
7. A special utility program is run to check whether the DEM represents the reservoir bottom topography or the water surface in the reservoir. If the DEM represents the reservoir bottom topography, the procedure skips the step 8 and continues with the step 9.
8. If the DEM represents the reservoir surface, remove automatically the water surface and the dam topography from the DEM. Estimate the bathymetry using a special utility program and burn it into the DEM. Continue the procedure with step 10.
9. Since the DEM already contains the bottom topography just perform dam removal using a special utility program.
10. Remove all the bridges given in the XML file from the DEM using the same utility program used in step 4.
11. Create the Manning's roughness map for the extent of the DEM using the classified remote sensing image and the vegetation index for the same area.
12. Create all the input files and then launch the simulation using CCHE2D-FLOOD.

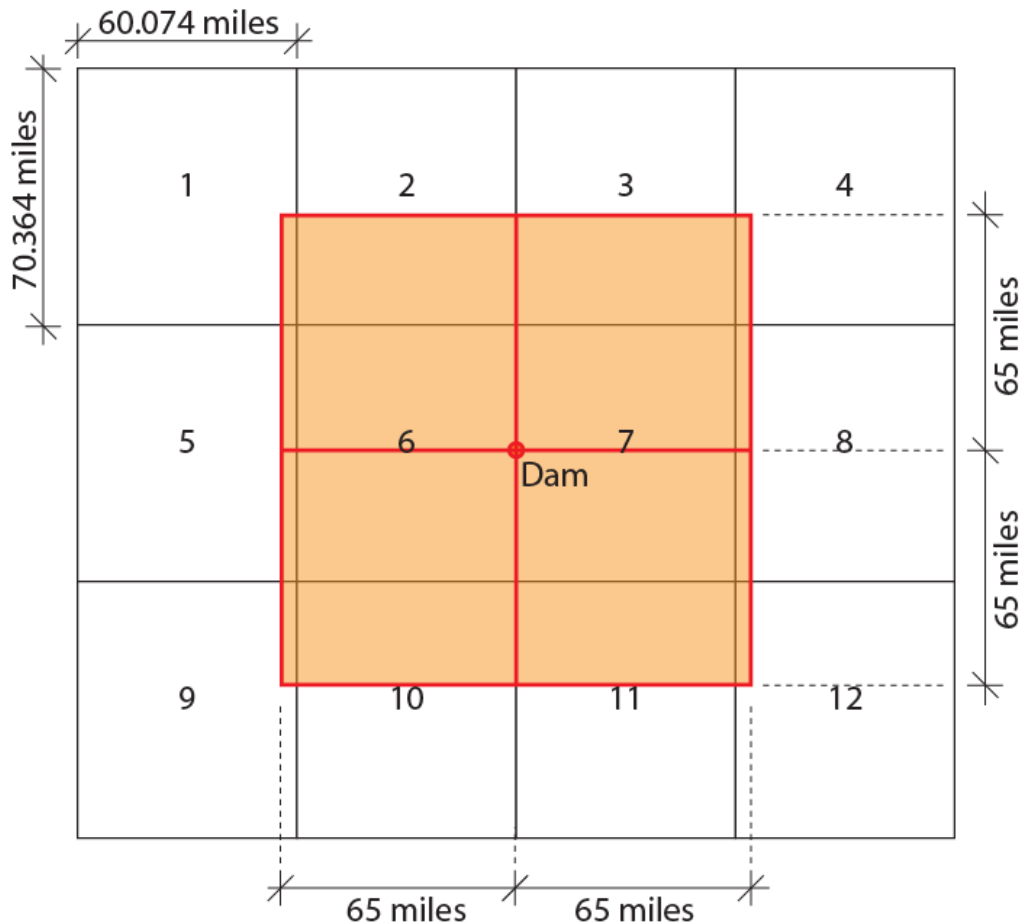


Figure 7. Clipping of the computational domain (shaded area) from DEM tiles.

The above procedure heavily relies on various utility programs to remove the bridges from the DEM, to remove the water surface and the dam from the DEM and to estimate the unknown reservoir bottom topography, etc. A detailed discussion of the algorithms is too involved and out of the scope of the present paper. Only some of the most important utility programs are here briefly.

4.2.3 Estimation of Bottom Topography of the Reservoir

The example used in the present paper to demonstrate various functionalities of the DSAT-DSS-WISE link is the test case for simulating a dam-break flood for the Dexter Dam in Oregon. The bottom topography is not available. In the 10m-resolution DEM, the lake appears as an almost flat surface. In fact, the case of the Dexter Reservoir involves an additional difficulty due to the fact that the road connecting Lowell, Oregon, to the Willamette Highway (Hwy 58) crosses the reservoir (Figure 8).

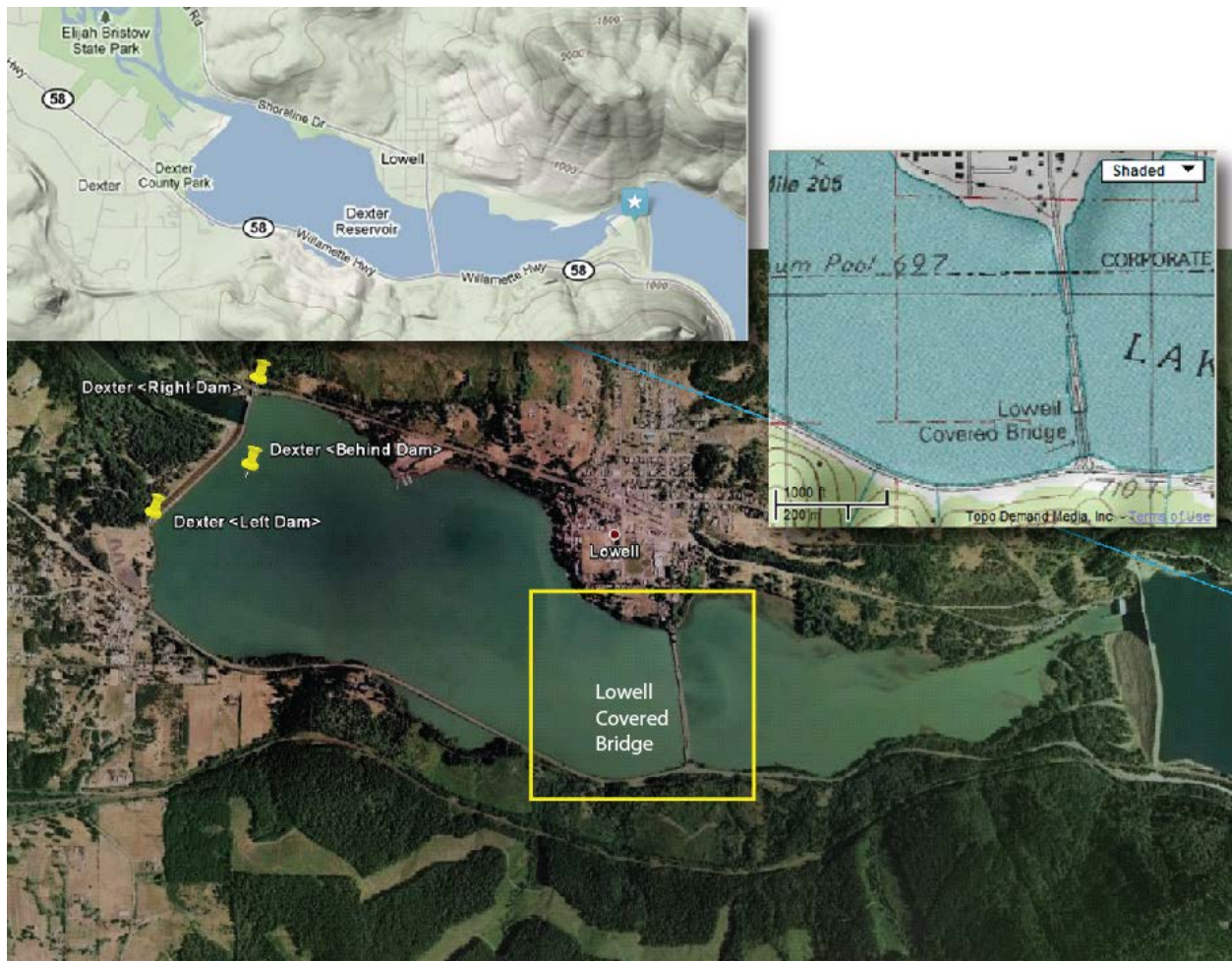


Figure 8. Satellite view of the Dexter Dam, Oregon, and the Lowell Covered Bridge.

Figure 9 shows the sequence of operations needed to replace the dam and the flat reservoir surface by an estimated bottom topography, which is later filled with water to reflect the initial conditions at the time of the failure, i.e. the beginning of the dam-break simulation. Referring to this figure, the general procedure can be described as follows:

- a. Identify the DEM cells inside the dam and the reservoir. If there are any bridges over the reservoir, the cells corresponding to the bridge opening must be lowered to create a gap.
- b. Remove the dam and reservoir from the DEM
- c. Calculate distance to shore for every cell. The "shore" for each cell is the nearest cell that was not determined to be part of the reservoir in step (a).
- d. Calculate the neighbor index for each cell in the reservoir. The neighbor index is a measure of likelihood for being far away from shore, and is determined by comparing the shore distance of a cell to each of its neighbors. If this cell is more distant from shore than a neighbor, the value of the neighbor index is increased by 1. If the cell is equally distant from shore as a neighbor, the index is increased by 1/2. Thus the neighbor index is between 0 and 4.
- e. Calculate centerline distance for each cell. Any cell with a neighbor index of 3.5 or greater is considered to be a "centerline cell". These cells are more distant

from shore than almost all their neighbors, and thus are likely to be towards the middle of the reservoir. Since the shape of the reservoir is unknown, and since it may contain any number of branches or curves, this procedure is an essential step for the estimation of the bottom topography.

- f. A predictor-corrector type procedure is used to fit a family of power curves (see Figure 10) to estimate the elevation of the bottom cells of the reservoir. The shapes of the power curves are adjusted until the computed volume is close to the volume given in the XML file.

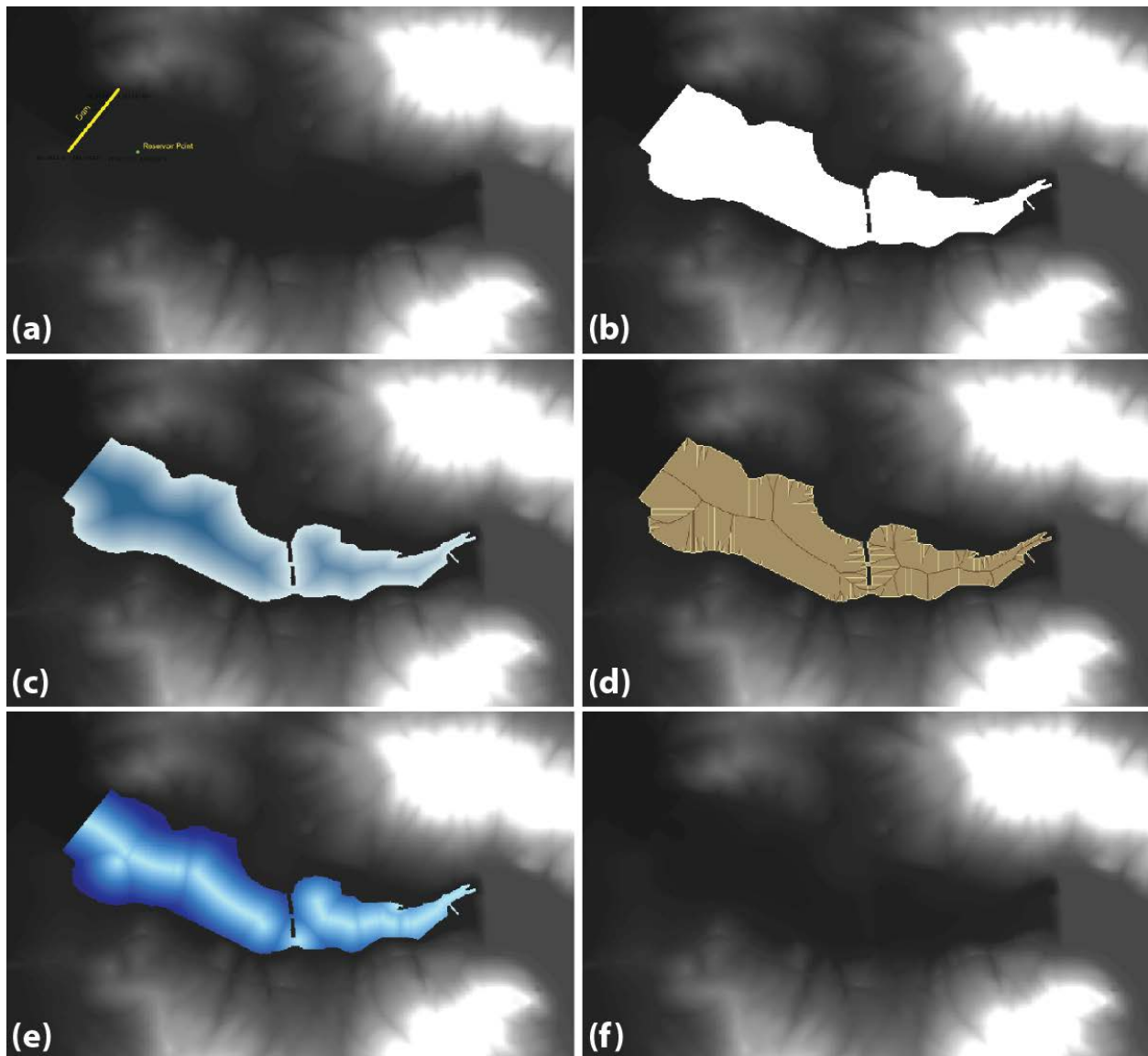


Figure 9. Steps for removing the water surface and the dam from the DEM and replacing it with estimated bottom topography. The case represented in this figure involves an additional level of difficulty due to the presence of a bridge over the reservoir.

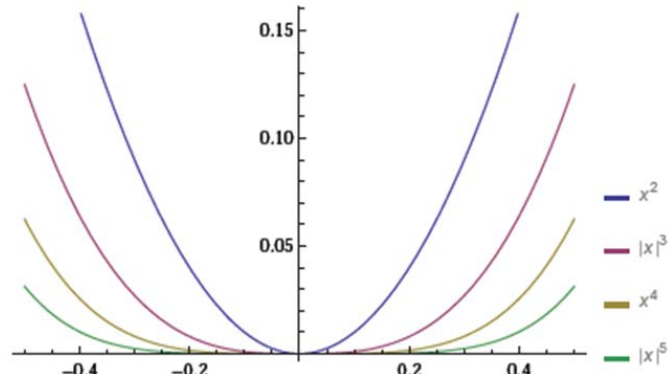


Figure 10. Power curves used in approximating the shape of the cross sections of the unknown reservoir bottom topography.

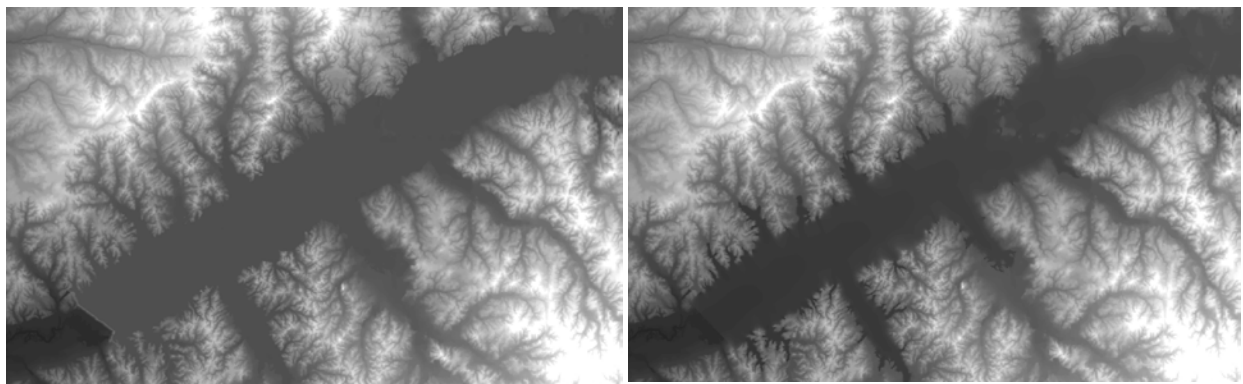


Figure 11. Estimation of the bathymetry of the Sardis Reservoir, Mississippi. Left: Original DEM showing a flat reservoir surface. Right: DEM with estimated bottom topography of the reservoir.

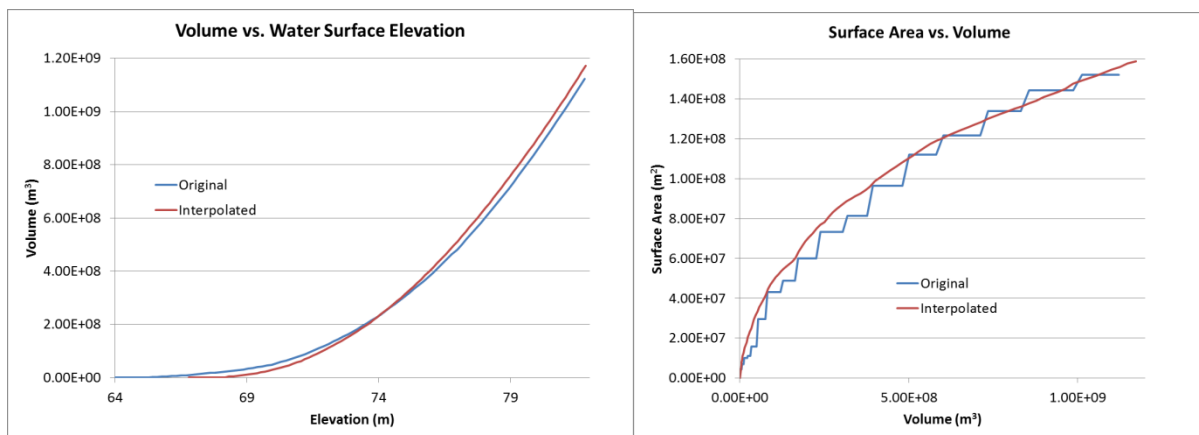


Figure 12. Comparison of the storage volume and the reservoir surface obtained from the estimated bottom topography of the reservoir with the true storage volume and reservoir surface.

The method was tested using the data from various reservoirs with known bathymetry. Figure 11 shows the original DEM and the DEM with the estimated bottom topography for the Sardis Dam, Mississippi. The true bottom topography of the Sardis Dam was

digitized from detailed bathymetry contours found in fishing maps. Figure 12 compares the storage volume versus water surface elevation and surface area versus storage volume curves obtained from the estimated bottom topography (interpolated) and the true bottom topography (original). As it can be seen, the agreement is remarkably good.

4.2.4 Automatic Bridge Removal

The road and railroad embankments can be quite high. Since the bridge openings and culverts under the crown elevation of the road cannot be represented in a DEM, in a flood simulation, the road and railroad embankments can act like linear features that prevent water passing from one side to the other. This may lead to errors in simulated flood depths, flood arrival times, and the extent of the inundation area. Figure 13 shows an extreme example where the railroad embankment downstream of the Little Seneca Dam in Montgomery County, Maryland, crosses the valley downstream almost at the same level as the dam crest.

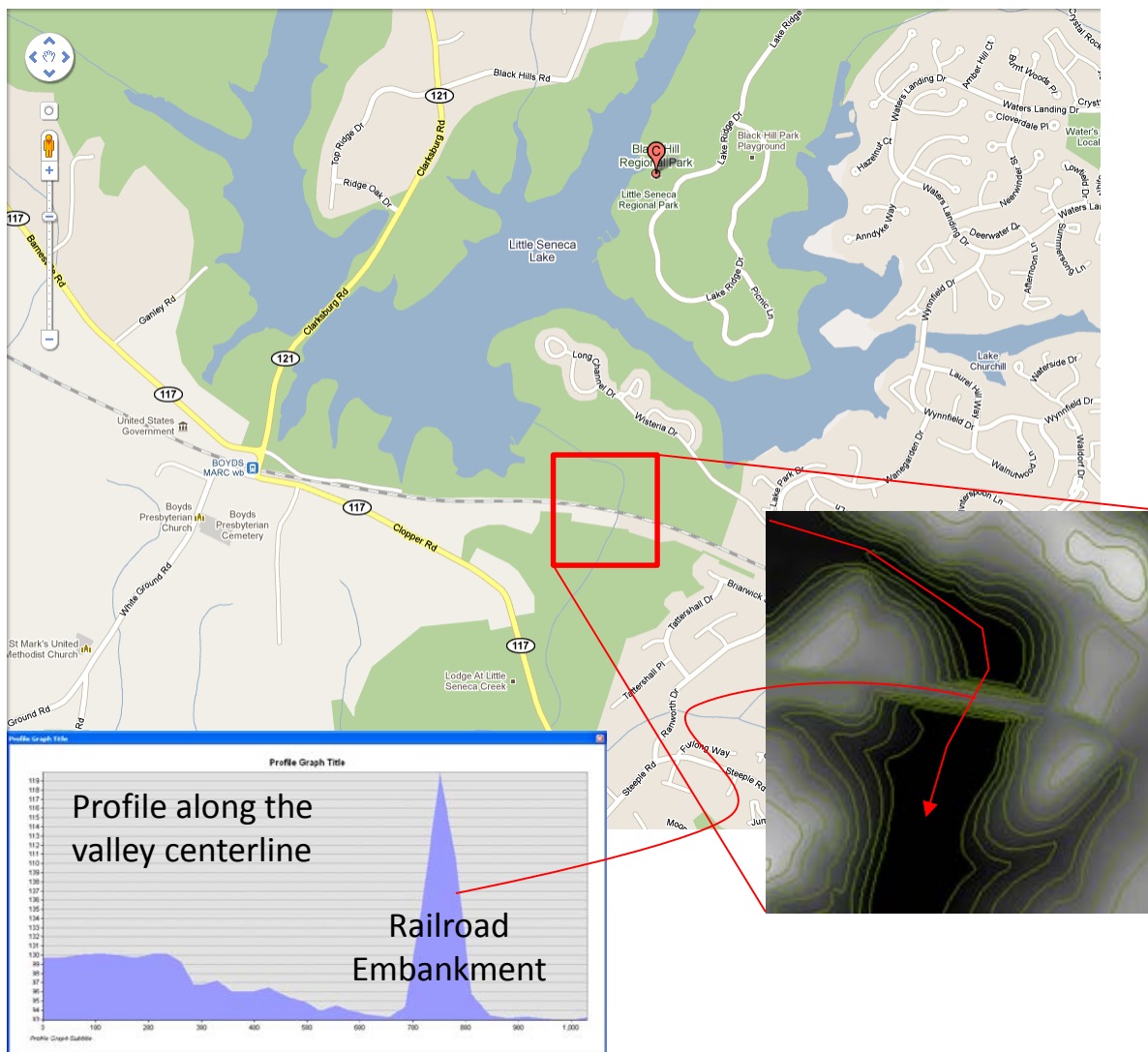


Figure 13. Railroad embankment downstream of the Little Seneca Dam, Maryland.

The XML file received from DSAT Viewer includes the bridge centerline locations and opening widths specified by the user. A special utility program uses this data to remove the bridges specified in the XML file by creating a breach in the embankment. The width of the breach is approximately equal to the width of the bridge opening.

The simple procedure adopted in the present case begins by drawing a circle around the center of the bridge with a diameter equal to the diameter of the bridge. The cell with the lowest elevation along the perimeter of the bridge is detected. This cell is assumed to represent the thalweg elevation of the channel bed. The cell at the center of the circle is then assumed to have the same elevation and the elevation of all the other points in the circle are interpolated using “*inverse distance weighting*” interpolation based on the center point and the points surrounding the circle. The application of this methodology to remove the bridge under the railroad embankment downstream of the Little Seneca Dam is shown in Figure 14.



Figure 14. Removal of the bridge under the railroad embankment downstream of the Little Seneca Dam. Left: original DEM; Right: DEM after bridge removal.







4.2.5 Automatic Assignment of the Manning’s Roughness Coefficient

The frictional energy loss term on the right hand side of momentum equations (see Eq. 9 and 12) contains the Manning’s roughness coefficient, n . Since the Manning’s roughness coefficient depends on the surface characteristics of the terrain, such as the land-use and land-cover properties, the CCHE2D-FLOOD allows the user to specify the distribution of the Manning’s coefficient over the computational domain. Hossain et al. (2009), proposed a methodology to assign the values Normalized Difference Vegetation Index (NDVI) based land use land cover (LU/LC), which was generated using the Landsat 5 Thematic Mapper (TM) and Advance Land Observing Satellite (ALOS) Panchromatic Remote-sensing Instrument for Stereo Mapping (PRISM) imagery. Manning’s roughness values corresponding to different remote sensing derived LU/LC features were obtained from published literature. This procedure, however, requires human intervention.

Since DSAT-DSS-WISE link operates without human intervention, the distributed Manning's roughness coefficients are assigned based on the National Land Cover Dataset 2006 (NLCD 2006), which is a 19-category land cover classification scheme that has been applied consistently over the conterminous U.S. The data has 30m resolution (http://www.mrlc.gov/nlcd_2006.php). Released by USGS in 2011, NLCD 2006 was constructed in a five-year collaborative effort by the 11-member federal interagency Multi-Resolution Land Characteristics Consortium (MRLC). NLCD 2006 data portrays 19 classes of land cover in the lower 48 states and the degree of surface imperviousness in urban areas. It is based on unsupervised classification of Landsat satellite imagery taken in 2006 (<http://www.usgs.gov/newsroom/article.asp?ID=2704>). The land cover color classification legend is shown in Figure 15.

NLCD has been used by many researchers to assign Manning's roughness values based on the land-cover (see Usery et al. 2004, Kalyanapu et al. 2009). The Manning's roughness values used by Kalyanapu et al. (2009) for some of the NLCD 2006 land cover types are listed in Table 1. Currently these values are also used to assign the distributed roughness values for the dam-break simulation requests sent by DSAT Viewer. During the clipping of the computational domain, the corresponding area is also extracted from the NLCD 2006 database. A utility program is written to generate a map of Manning's roughness values based on the land-cover type using the values in Table 1. Additional work is currently under way to verify and validate these values.

NLCD Land Cover Classification Legend

	11 Open Water
	12 Perennial Ice/Snow
	21 Developed, Open Space
	22 Developed, Low Intensity
	23 Developed, Medium Intensity
	24 Developed, High Intensity
	31 Barren Land
	41 Deciduous Forest
	42 Evergreen Forest
	43 Mixed Forest
	51 Dwarf Scrub*
	52 Shrub/ Scrub
	71 Grassland/ Herbaceous
	72 Sedge/ Herbaceous *
	74 Moss *
	81 Pasture Hay
	82 Cultivated Crops
	90 Woody Wetlands
	95 Emergent Herbaceous Wetlands

* Alaska Only

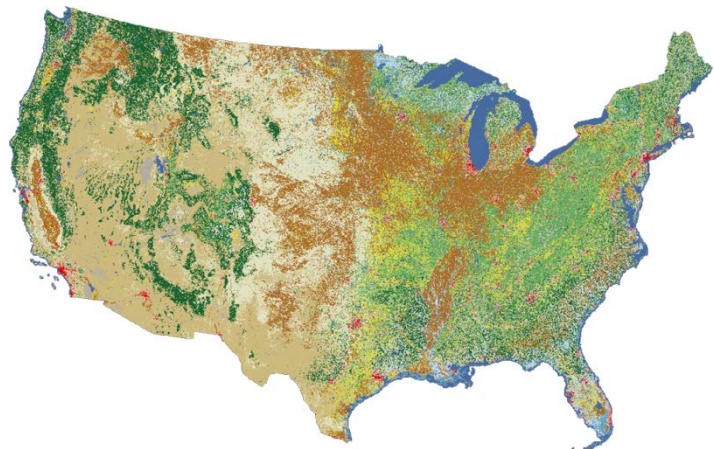


Figure 15. The land cover color classification legend. The definition of classes can be found in http://www.mrlc.gov/nlcd_definitions.php.

Table 1. Manning’s roughness coefficients for different NLCD 2006 land cover types as proposed by Kalyanapu et al. (2009).

Land Cover	Description	$n (m^{-1/3} s)$
21	Developed, open space	0.0404
22	Developed, low intensity	0.0678
23	Developed, medium intensity	0.0678
24	Developed, high intensity	0.0404
31	Barren land	0.0113
41	Deciduous forest	0.36
42	Evergreen forest	0.32
43	Mixed forest	0.4
52	Shrub/scrub	0.4
71	Grassland/herbaceous	0.368
81	Pasture/Hay	0.325
90	Woody wetlands	0.086
95	Emergent herbaceous wetlands	0.1825

4.3 Automatic Dam-Break Flood Simulation and Output Files

By burning in the estimated bottom topography of the reservoir and removing the bridges specified in the XML file, the digital topography clipped from the DEM tiles is converted into a computational grid that can be used for the simulation of the dam-break flood problem. Before the simulation can be launched, some additional task must be accomplished and the input files needed by the CCHE2D-FLOOD must be prepared:

- A utility program calculates the map of the initial water depths in the reservoir using the following information provided in the XML file: (1) coordinates of the dam axis end points A and B; (2) coordinates of the point in the reservoir (C); and (3) the pool elevation at the time of the failure.
- All the boundary cells along the four edges of the computational domain are declared as open boundary cells.

Once these two operations are completed, the input files for CCHE2D-FLOOD are automatically written and the computation is launched.

Computational domains automatically prepared following the procedure described above can be quite large even at 30m resolution. A parallelized multi-core, multi-threaded version of the CCHE2D-FLOOD is used to carry out the computations in a very short time. This version of the code uses a linked-list structure to track the cells that contain water. Rather than sweeping the entire computational grid, the computations are carried out only the wet (i.e. water containing) cells that are in the list. When a new cell receives water and becomes wet, it is added into the list. Conversely, cells that become empty are erased from the list. This implementation takes into

account the fact that during a simulation a large number of cells in the computational domain may not receive water; thus, they do not need to be computed.

Simulation results are sent to the user in the form of shape files that can be read and displayed by the DSAT Viewer: (1) a depth grid of the flood; and (2) a map of arrival times of the flood.

In the future, a second solver, called WGFEM, will also be used for carrying out the simulation for DSAT-DSS-WISE link. WGFEM uses GPGPU (General Purpose Graphics Processing Unit) technology to achieve unprecedented computational speeds, which can be as much as 30 to 100 times the computational speed that can be achieved on classical CPU-based numerical models of the same type. The server at the NCCHE has 3 NVidia Fermi C2070 6GB CUDA cards, each with a 448 streaming processors. Using these cards, the computations can be carried out very fast. The tests on the WGFEM solver are currently under way.

5. Conclusions

Advanced flood modeling computational tools developed at UM-NCCHE through the support provided by the DHS-sponsored SERRI Program at the Oak Ridge National Laboratory, are made available to Dams Sector stakeholders through the DSAT web-based tool that provides secure access to different modules and applications covering a wide range of analytical capabilities.

The capabilities developed at UM-NCCHE provide users of DSAT with a first-tier dam-break flood simulation. The computational domain and input data are prepared automatically based on a minimum amount of basic information prepared using a graphical user interface implemented on DSAT. Simulations are carried out on a dedicated server at UM-NCCHE at faster-than-real-time speeds. The results are sent back to DSAT for viewing and analysis.

It is important to note that the automatic dam-break analysis provides only a first-tier simulation for quickly assessing the dam safety issues involved. It does not replace detailed studies that should normally be carried out by professional engineers with hydraulics and hydrology background and specialization in numerical modeling techniques.

References

1. Altinakar, M.S., Matheu, E. E. and McGrath, M. (2009): "New Generation Modeling and Decision Support Tools for Studying Impacts of Dam Failures", Proceedings of the ASDSO Dam Safety 2009 Annual Conference, September 27-October 1, 2009, Hollywood, FL.
2. Godunov S. (1976), Résolution numérique des problèmes multidimensionnels de la dynamique des gaz (Editions de Moscou).
3. Graham, W.J. (1999): "A Procedure for Estimating Loss of Life Caused by Dam Failure", Report No. DSO-99-06, Dam Safety Office, US Bureau of Reclamation, Denver, CO.
4. Harten, A., Lax, P., and van Leer, B. (1983): "On upstream differencing and Godunov type methods for hyperbolic conservation laws"; SIAM review. 25(1), pp 35-61.
5. Hossain, A.K.M.A.; Jia, Yafei, and Chao, Xiabo (2009): "Estimation of Manning's roughness coefficient distribution for hydrodynamic model using remotely sensed land cover features"; Geoinformatics, 2009 17th International Conference on Volume , Issue , 12-14 Aug. 2009 Page(s):1 – 4 / Digital Object Identifier, 10.1109/GEOINFORMATICS.2009.5293484
6. Kalyanapu, Alfred J., Burian, Steven J., and McPherson Timothy N. (2009). "Effect of land use-based surface roughness on hydrologic model output", Journal of Spatial Hydrology, Vol.9, No.2 Fall
7. Kim, Dae-Hong, Cho, Yong-Sik, and Yong-Kon, Yi (2007): "Propagation and Run-up of Nearshore Tsunamis with HLLC Approximate Riemann Solver"; Ocean Engineering, Volume 34, Issues 8-9, June, Pages 1164-1173.
8. RESCDAM. 2000. The use of physical models in dam-break flood analysis. Rescue actions based on dam-break flood analysis. Final report of Helsinki University of Technology, Helsinki, Finland. 57 p.
9. Toro, E.F. (2010): *Riemann solvers and numerical methods for fluid dynamics*. Springer, Third Edition, 2010.
10. Toro, E.F., Spruce, M. and Spears, W. (1994): "Restoration of the Contact Surface in the HLL Riemann Solver"; Shock Waves, Vol. 4, pp: 25-34.
11. USACE. 1985. Business depth damage analysis procedure, Engineer Institute for Water Resources. Research Report 85-R-5. Portland, Oregon. 100 p.
12. Usery, E. L., Finn, M. P., Scheidt, D. J., Ruhl, S., Beard, T., and Bearden, M. (2004). "Geospatial data resampling and resolution effects on watershed modeling: A case study using the agricultural non-point source pollution model." Journal of Geographic Systems, 6, 289-306.